J Mater Sci (2011) 46:727–733
DOI 10.1007/s10853-010-4803-y

Microstructure and toughness of coarse grain heat-affected zone of domestic X70 pipeline steel during in-service welding

Chaowen Li · Yong Wang · Tao Han · Bin Han · Liying Li

Received: 5 June 2010 / Accepted: 27 July 2010 / Published online: 7 August 2010

Abstract The microstructures and mechanical properties of coarse grain heat-affected zone (CGHAZ) of domestic X70 pipeline were investigated. The weld CGHAZ thermal cycles having different cooling time $\Delta t_{8/5}$ were simulated with the Gleeble-1500 thermal/mechanical simulator. The Charpy impact absorbed energy for toughness was measured, and the corresponding fractographs, optical micrographs, and electron micrographs were systematically investigated to study the effect of cooling time on microstructure, impact toughness, and fracture morphology in the CGHAZ of domestic X70 pipeline steel during in-service welding. The results of simulated experiment show that the microstructure of CGHAZ of domestic X70 pipeline steel during in-service welding mainly consists of granular bainite and lath bainite. Martensite–austenite (M–A) constituents are observed at the lath boundaries. With increase in cooling time, the M–A constituents change from elongated shape to massive shape. The reduction of toughness may be affected by not only the M–A constituents but also the coarse bainite sheaves. Accelerating cooling with cooling time $\Delta t_{8/5}$ of 8 s can be chosen in the field in-service welding X70 pipeline to control microstructures and improve toughness.

Introduction

The high strength and good toughness pipeline steels have been widely used in oil and natural gas transport engineering and have made a contribution to pipeline cost savings, especially for long-distance high-pressure pipelines [1]. The Chinese West-East Natural Gas Transporting project in which the X70 acicular ferritic pipeline steels were used greatly promotes domestic studies of the high strength and toughness pipeline steels [2–4]. Because of the small effective grain size with high angle boundaries, high density of dislocations, and chaotic structure, acicular ferrite (AF) microstructure has the potential of combining high strength and high toughness [5]. This is because the plates of AF nucleate intragranularly on nonmetallic inclusions within large austenite grains, and then radiate in many different orientations from those inclusions while maintaining an orientation relationship with austenite [6].

The balance of high strength and good toughness in pipeline steels can be upset by the thermal cycles experienced during welding, producing poor toughness in the heat-affected zone (HAZ). Historically, the lowest toughness was expected in the coarse grain HAZ (CGHAZ), which is the part of the HAZ adjacent to the weld fusion line [7]. The increasing frequency of sour conditions within gas and oil pipelines increases the risks involved in welding on pressure-containing lines and imposes additional restraints in the form of maximum tolerable hardness, especially in the HAZ. The high rate of cooling, the hydrogen content of the weld metal, and elevated stress levels in the weld region all favored subsequent crack formation. During in-service welding pipeline, the flowing natural gas or oil creates a large heat loss through the pipe wall, resulting in accelerated cooling of the weld joints [8]. The rapid cooling has been reported [9] to significantly affect the HAZ microstructure and it also may increase hardness and promotes brittle microstructures which increase the susceptibility of cold cracking [10].

C. Li · Y. Wang (✉) · T. Han · B. Han · L. Li
College of Mechanical and Electronic Engineering,
China University of Petroleum,
Dongying 257061, China
e-mail: yongwang@upc.edu.cn

In the present study, domestic X70 pipeline steel specimens were prepared for investigation of in-service welding by varying cooling time. Charpy impact test was conducted on them in order to investigate the effects of rapid cooling on microstructure and fracture toughness.

Experimental procedures

Experimental material

The specimens were machined from domestic X70 pipeline steel with a diameter of 1016 mm and thickness of 21 mm. The chemical composition and mechanical properties are shown in Tables 1 and 2, respectively. Figure 1 presents the optical microscope (OM) microstructure of the domestic X70 pipeline steel. It can be seen that the microstructure is AF with polygonal ferrite (PF) and quasi-polygonal ferrite (QPF) dominated microstructures. The average grain size is about 10 μm and minimal grain is 3–5 μm. From Hall-Petch equation [11], the materials with small diameter of grain can be strengthened significantly by fine-crystal reinforcement, through which the toughness also can be increased.

Table 1 Chemical composition of domestic X70 pipeline steel (wt%)

Elements	Content
C	0.05
Si	0.26
Mn	1.48
S	0.003
P	0.012
Cr	0.027
Mo	0.17
Cu	0.22
V	0.052
Ni	0.15
Ti	0.016
Nb	0.05
Pcm	0.164
Ceq	0.404

Note: Pcm = C + (Mn + Cu + Cr)/20 + Mo/15 + V/10 + Si/30 + Ni/60; Ceq = C + (Mn + Si)/6 + (Ni + Cu)/15 + (Cr + Mo + V)/5

Table 2 Mechanical properties of domestic X70 pipeline steel

Yield strength, σ_s (MPa)	Tensile strength, σ_b (MPa)	Elongation, δ (%)	Absorbed energy, A_{kv} (−20 °C, J)
570	650	31	252

Experimental method

In fact, the CGHAZ in a welded joint is too narrow, so that it is sometimes impossible to get available test specimens. To overcome this problem, welding thermal cycle simulation technique was applied in this study. Since simulated HAZ tests give the same toughness ranking, although not the same absolute values [12], as those on actual welding HAZ, a simulated CGHAZ can be used to substitute for an actual CGHAZ.

The thermo-mechanical simulation was conducted in a Gleeble-1500 thermal/mechanical simulator. Square bar specimens (10.5 mm × 10.5 mm × 80 mm) for thermal cycle simulation were cut with the longitudinally along the rolling direction. The simulated thermal cycles were schematically shown in Fig. 2. The CGHAZ thermal cycle was designed to simulate a manual arc welding of approximately 1.2 kJ/mm heat input in different thick pipe.

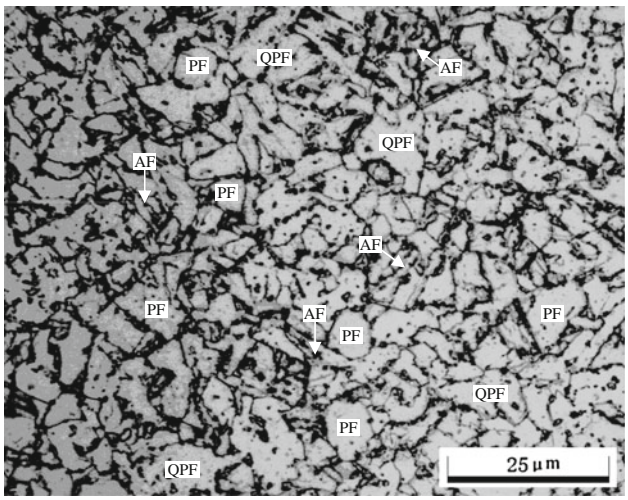

Fig. 1 Optical microstructure of X70 pipeline steel

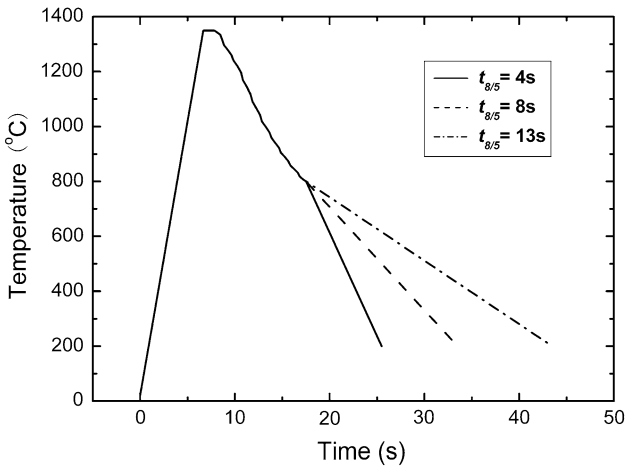

Fig. 2 Curves of weld thermal cycle used in experiment

This involved heating to a peak temperature of 1350 °C at a rate of approximately 200 °C/s and holding at the peak temperature for 1.2 s. The most important thermal cycle parameter for a fixed peak temperature (taken as 1350 °C for the CGHAZ) is the cooling rate. The cooling rate is usually specified as the cooling time from 800 to 500 °C ($\Delta t_{8/5}$) and can be related to welding heat input. As the research by Ikawa et al. [13] shows that cooling condition below 500 °C also exerts some influence on toughness, therefore the temperature was controlled until it fell to 200 °C. After the welding HAZ thermal cycle was applied, specimen was subjected to the Charpy impact test to evaluate the toughness of simulated CGHAZ. For convenience, absorbed energy at −20 °C was employed as a measure of HAZ toughness. In order to elucidate the relationship between strength and toughness of CGHAZ, microhardness tests were performed using a Vickers pyramidal indenter with an indenting force of 200 g.

In order to characterize the microstructure of the base metal and the CGHAZ, the optical micrographic specimens were prepared by conventional grinding and polishing techniques and etched with 4 vol% Nital solution for revealing the microstructure. The microstructural features were observed with an NIKON EPIPHOT 300U OM. Then, slices were cut along the cross-section in the middle of specimens with spark cutting and polished by the precision ion polishing system with the type GL-6960. Thin foils were observed in an H-800 transmission electron microscope (TEM) at 150 kV operating voltage. After the thermo-mechanical process, the simulated specimens were cut and ground to the standard Charpy size of 5 mm × 10 mm × 55 mm. Notch was located in the uniform microstructural region at the center of thermo-mechanically treated specimens. Charpy impact testing (INSTRON WOLPERT PW30) was carried out at the temperature of −20 °C for a measure of HAZ toughness. The fracture morphology was observed in a scanning electron microscope (SEM, JEOL JSM-6380LA).

Results and discussion

Relations between microstructures and cooling time

The optical micrographs of CGHAZ obtained from thermal cycle simulation are shown in Fig. 3. It can be found that the grain size of CGHAZ was larger compared to the original one (Fig. 1) for the effect of thermal circle. The specimens treated in different cooling time show great differences in grain size and microstructure morphology. When cooling time, $\Delta t_{8/5}$, is 4 s, the cooling rate was fast enough to get some acicular structure before the displacive transformation occurred and preserve small austenite grain size (Fig. 3a), which can overcome the reduction in

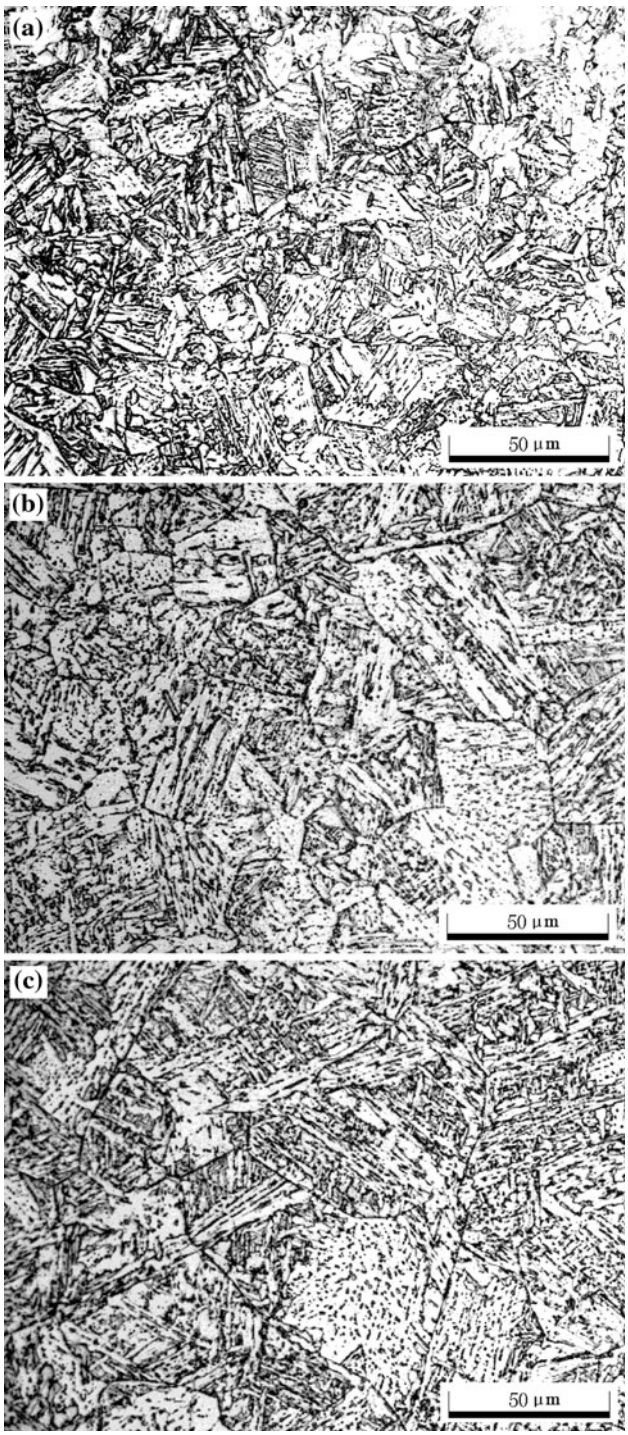

Fig. 3 Typical microstructure of CGHAZ with different cooling time **a** $\Delta t_{8/5}$ of 4 s, **b** $\Delta t_{8/5}$ of 8 s, **c** $\Delta t_{8/5}$ of 13 s

fracture toughness [14]. It appears that the fast cooling rate has led to a chaotic microstructure. On the other hand, with the increase of cooling time, $\Delta t_{8/5}$, the specimens give a clear sheaf-like bainitic structure (Fig. 3b, c). There are high volume fractions of sheaf-like bainitic structure with a few amounts of M–A constituents. The sub-unit platelets of

sheaf-like bainitic structure are fine. Figure 4 illustrates transmission electron micrographs and corresponding diffraction pattern of the M–A constituents. Being irregular in shape and size in micros, these M–A constituents are located at the lath boundaries (Fig. 4a, b). The selected area diffraction pattern shown in Fig. 4c was taken from this area, which is seen to be superimposed by several single diffraction patterns. The scanning electron micrograph in Fig. 5 reveals the morphology of microstructure for the corresponding optical micrograph shown in Fig. 3. It clearly shows that the major microstructures of CGHAZ are granular bainite and lath bainite with a large prior austenite grain size. Prior austenite grain boundaries are distinct in the CGHAZs.

For pipeline steel, on cooling from austenite state, austenite first transforms into polygonal ferrite during the continuous cooling, and then carbon concentrates in the retained austenite. When the carbon-rich austenite is cooled to a temperature below the martensite start temperature (M_s), it will partially transform to martensite and forms the M–A constituents. Hence, the amount of M–A constituents is related to the critical carbon content of the residual austenite where the bainite or acicular transformation ceases [15, 16]. Cooling time has very strong influences on the microstructures of the pipeline steels. With decreasing the cooling time, the amount of lath bainite decreases greatly while the granular one increases obviously. The morphology, quantity, and size of the M–A constituents also vary a lot with the cooling time, as shown in Fig. 4. That is, this constituent is observed as elongated rods at short cooling time (Fig. 4a). As the cooling time increases, this changes into massive (Fig. 4b). Carbon concentration distribution in the interface is different according to the change of cooling time. When the cooling time, $\Delta t_{8/5}$, is 13 s, some part of M–A constituent decomposes into ferrite and carbide, in the temperature range of 300–350 °C. If cooling is rapid enough ($\Delta t_{8/5} = 4$ s), this decomposition dose not happen. Then, during the cooling course afterwards, part of the retained austenite with high-carbon content transforms to martensite plates with different size and orientation when the temperature reaches M_s. Then M–A constituent is formed at the boundaries of bainite [17]. The above analysis can thus explain the effects of cooling time on the amount of M–A constituent. The existence of M–A constituent causes a detrimental effect on toughness. Reduction in the amount of the M–A constituent will decrease the ductile–brittle transition temperature and will also promote the toughness of the steel [6].

The transmission electron microstructure in Fig. 6 for the fine structure of the CGHAZ reveals the predominantly acicular lath structure. All the specimens exhibited irregular acicular laths and the morphology of this substructure unit varies according to the cooling time. Conventional

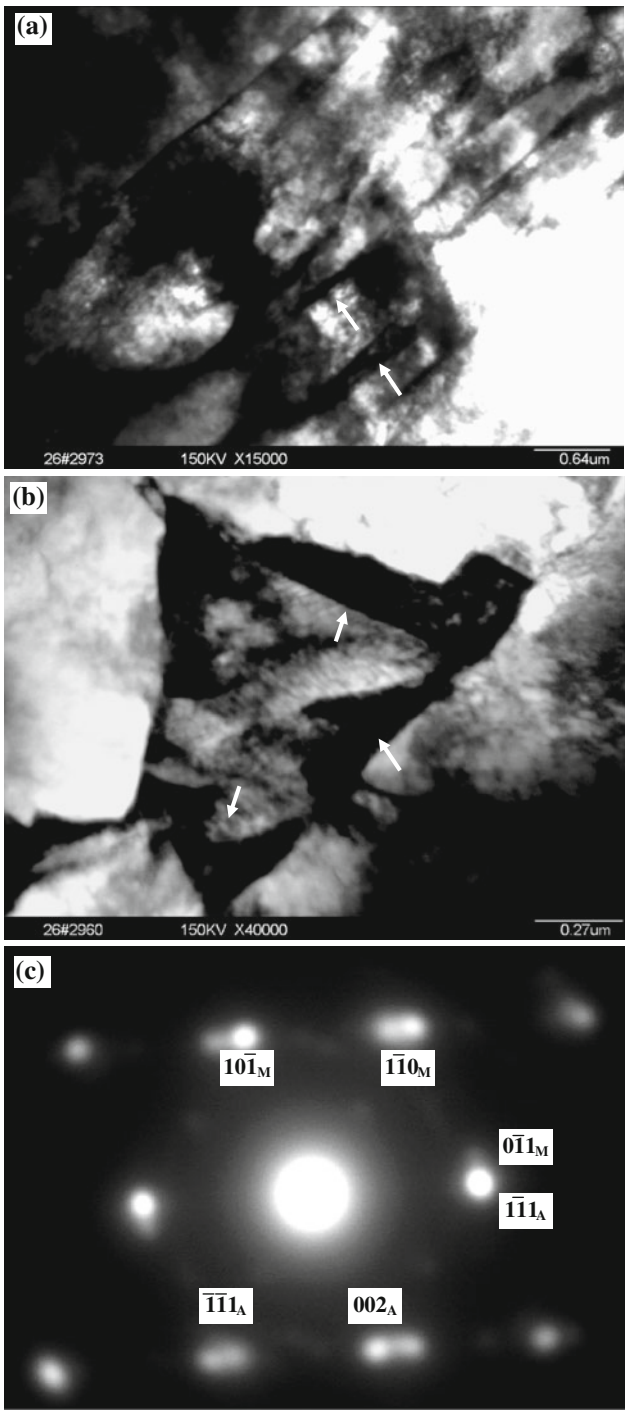

Fig. 4 TEM images of the fine structure of M–A constituent: **a** elongated M–A constituent ($\Delta t_{8/5} = 4$ s), **b** massive M–A constituent ($\Delta t_{8/5} = 8$ s), **c** micro-diffraction pattern of M–A constituent

SEM characterization may provide the ability to observe acicular lath width. The average acicular lath width of specimen with cooling times, $\Delta t_{8/5}$, of 8 s and 13 s are 0.7–0.8 μm and 1.5–1.6 μm, respectively. It can be noted that width of ferrite lath increases with the increase of cooling time. The size of substructure caused by an

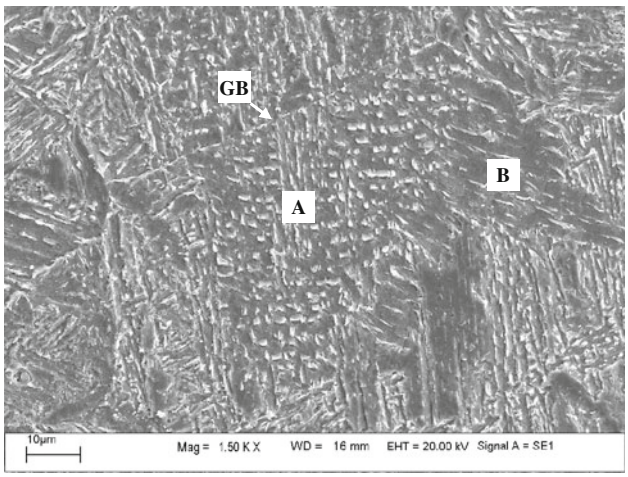

Fig. 5 SEM micrograph of CGHAZ: prior-austenite grain boundary (*GB*) indicated by *white arrow*, granular bainite (*A*), and lath bainite (*B*)

increase in the width of lath sheave has some effect on toughness in case of short cooling time, because the boundaries of laths can be an impediment against brittle fracture. The granular bainite has a function of segmentation lath bainite and lets the lath bainite with the same orientation become thinner and shorter. The boundary of the lath can play a role similar to that of the grain boundary. When crack propagates to the boundary of the lath, it will be bent which can efficiently hinder the propagation of the crack and improve the toughness [18].

Relations of toughness and hardness with cooling time

The relations of absorbed energy and hardness of the CGHAZ with cooling time, $\Delta t_{8/5}$, are shown in Fig. 7. It can be seen from the figure that the absorbed energy is the highest with $\Delta t_{8/5}$ of 8 s, while it is still lower than that of the base metal with the absorbed energy of 252.2 J. The absorbed energy decreases when $\Delta t_{8/5}$ is shorter than 8 s. When $\Delta t_{8/5}$ is longer than 8 s, the absorbed energy remains decreasing. Hardness is an important factor for evaluating cold cracking resistance. It can be also seen from Fig. 7 that the hardness is much higher than that of the base mental with decreasing the cooling time, suggesting that the susceptibility to cold cracking may be high. Thus, choosing appropriate heat input during in-service welding is important in order to obtain better toughness and suitable hardness which is beneficial to preventing hydrogen.

Due to the effect of thermal cycle with high peak temperature, most of particles, such as V (C, N), Nb (C, N) dissolve into the steel, which weakens the pinning effect of the grain boundaries and loses the function of controlling the grain coarsening. It leads to the abnormal growth of the grains in the CGHAZ, and the grains will be more coarsen

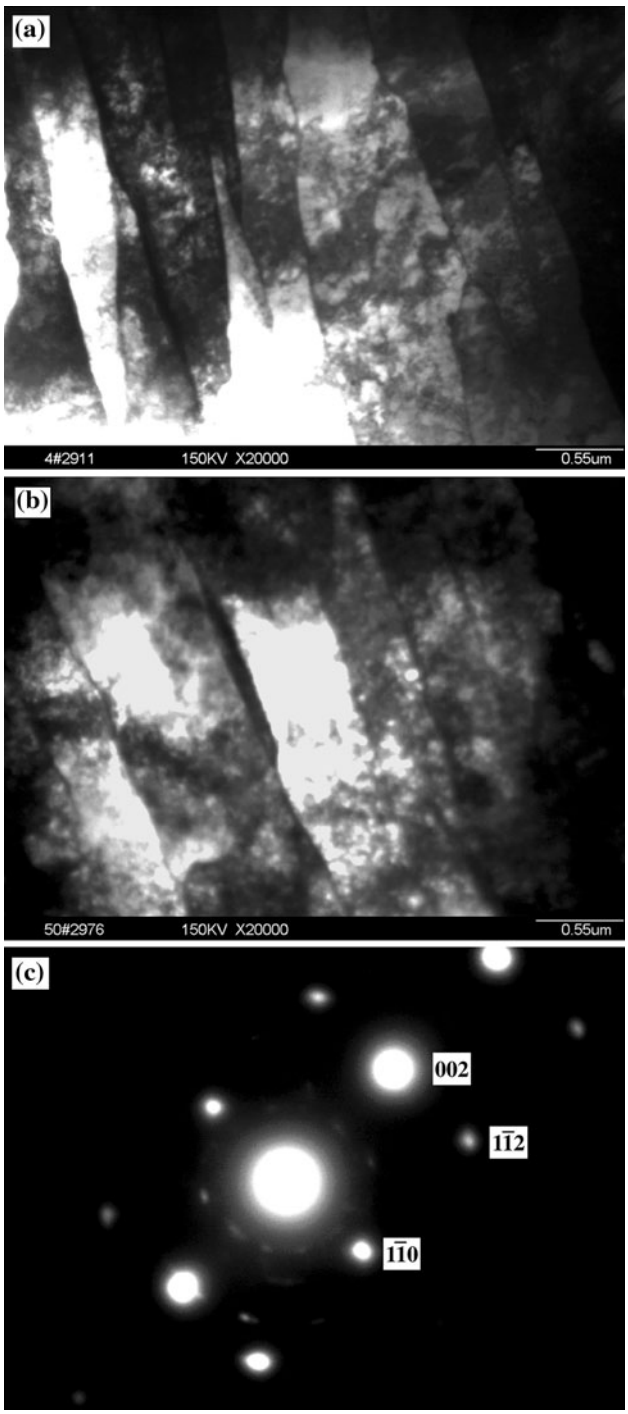

Fig. 6 Typical structure of ferrite laths with different cooling time **a** $\Delta t_{8/5}$ of 8 s, **b** $\Delta t_{8/5}$ of 13 s, **c** micro-diffraction pattern of ferrite lath

and the toughness will apparently decrease with the increase in the cooling time. The reason for good toughness of the specimen with $\Delta t_{8/5}$ of 8 s is that the microstructure is composed of a great amount of granular bainite and retained austenite films which have good toughness. The retained austenite films mainly disperse at bainite grains boundaries or at substructure boundaries. Besides the

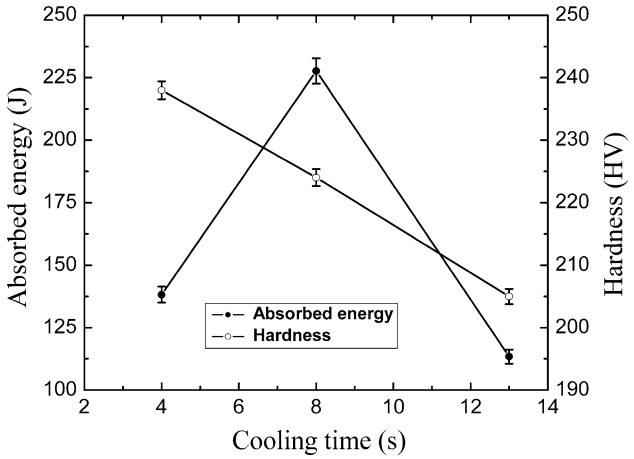

Fig. 7 Change of absorbed energy and hardness versus cooling time

microstructure morphology, proportion, size and distribution of the M–A constituents also directly affect the toughness of the granular bainite.

Under the condition of fast cooling, the carbon in the CGHAZ of X70 pipe steel has no enough time to diffuse. The carbon exists in the remained austenite in the state of supersaturated and transformed with the austenite to bainite during the middle temperature. Compared to the ferrite, the bainite has high carbon amount and large amount of lattice deficiencies. As a result, it has high hardness. With the increase of the cooling time, the hardness of the microstructure in the CGHAZ has a decrease tendency. On one hand, the microstructure morphology gradually changes from lath bainite to granular bainite and the M–A constituents are fine and dispersive. On the other hand, with the decrease of the cooling time, the amount of ferrite in the microstructure increases while the amount of bainite gradually decreases. The two reasons combine to cause the decrease of the hardness.

Fracture morphology

The fractographs of impact specimen are studied by SEM. Figure 8 shows the detailed fracture morphology for three different cooling time specimens. The fracture mode of the specimen with $\Delta t_{8/5}$ of 4 s (Fig. 8a) is primarily cleavage, associated with small and poorly defined facts connected to ductile tear ridges. A slight river patter can be seen radiating from the facet center. It can be seen that ductile fracture is present in the specimen with $\Delta t_{8/5}$ of 8 s (Fig. 8b). The fracture appearance of the specimen with $\Delta t_{8/5}$ of 13 s (Fig. 8c) reveals irregular facets separated by heavy ridges. Within the cleavage, many parallel branches of the river pattern are present. These results provide a convincing evidence to suggest that appropriate cooling time can improve the CGHAZ toughness.

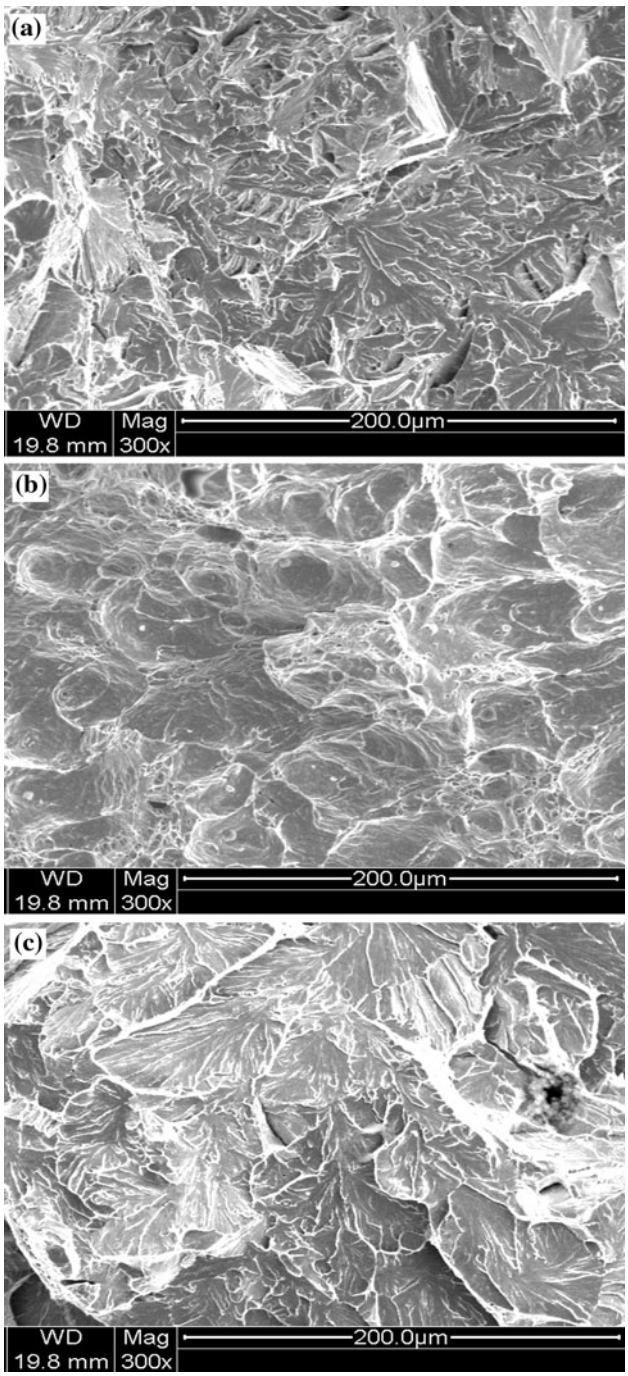

Fig. 8 Fractographs of simulated CGHAZ for Charpy impact specimens with different cooling time **a** $\Delta t_{8/5}$ of 4 s, **b** $\Delta t_{8/5}$ of 8 s, **c** $\Delta t_{8/5}$ of 13 s

Conclusions

In this study, microstructure, toughness, and fracture morphology of CGHAZ of the domestic X70 pipeline steel were studied mainly from the viewpoint that accelerated cooling rate caused by in-service welding. It is shown that the major microstructures of CGHAZ of domestic X70

pipeline steel during in-service welding are granular bainite and lath bainite. M–A constituent also can be found at the lath boundaries in the CGHAZ during rapid cooling. With increasing in cooling time, the M–A constituent changed from elongated shape to massive shape and the absorbed energy of Charpy impact test of CGHAZ of X70 pipe steel was first increased and then decreased. When the cooling time, $\Delta t_{8/5}$, is 4 s and 13 s, the toughness decreased in large amplitude. The authors think that the absorbed energy of Charpy impact test may be affected not only by M–A constituents but also by coarse bainite sheaves.

Acknowledgements The authors would like to acknowledge the supports of Innovation Fund for Doctors of China University of Petroleum (B2009-13).

References

1. Ouchi C (2001) ISIT Int 41(6):542
2. Wang W, Shan Y, Yang K (2009) Mater Sci Eng A 502(1–2):38
3. Yu H (2008) J Univ Sci Technol Beijing 15(6):683
4. Zhao Z, Wang Z, Zhang H, Qiao L (2007) J Univ Sci Technol Beijing 14(5):410
5. Avazkonandeh-Gharavol M, Haddad-Sabzevar M, Haerian A (2009) J Mater Sci 44(1):186. doi:10.1007/s10853-008-3103-2
6. Chiou C, Yang J, Huang C (2001) Mater Chem Phys 69(1–3):113
7. Li Y, Crowther DN, Green MJW, Mitchell PS, Baker TN (2001) ISIJ Int 41(1):46
8. Wahab MA, Sabapathy PN, Painter MJ (2005) J Mater Process Technol 168(3):414
9. Sathiya P, Aravindan S, Soundararajan R, Noorul Haq A (2009) J Mater Sci 44(1):114. doi:10.1007/s10853-008-3098-8
10. Kitagawa Y, Ikeuchi K, Kuroda T, Matsushita Y, Suenaga K, Hidaka T, Takauchi H (2008) J Mater Sci 43(1):12. doi:10.1007/s10853-007-2150-4
11. Weertman JR (1993) Mater Sci Eng A 166(1–2):161
12. Qiu H, Mori H, Enoki M, Kishi T (2000) Metall Mater Trans A 31(11):2785
13. Ikawa H, Oshige H, Tanoue T (1980) Trans Jpn Weld Soc 11(2):3
14. Raj B, Saroja S, Laha K, Karthikeyan T, Vijayalakshmi M, Bhanu Sankara Rao K (2009) J Mater Sci 44(9):2239. doi:10.1007/s10853-008-3199-4
15. Wang S-C, Yang J-R (1992) Mater Sci Eng A 154(1):43
16. Shi Y, Han Z (2008) J Mater Process Technol 207(1–3):30. doi:10.1016/j.jmatprotec.2007.12.049
17. Taban E (2008) J Mater Sci 43(12):4309. doi:10.1007/s10853-008-2632-z
18. Shibata K, Asakura K (1995) ISIJ Int 35(8):982